# Numerical Modelling of Ultrasonic Phased Array Transducers and Their Application

Prashanth Kumar CHINTA, René MARKLEIN, University of Kassel, Department of Electrical Engineering and Computer Science, Electromagnetic Field Theory, Kassel, Germany
Walter DE ODORICO, Roman KOCH, Albrecht MAURER, GE Inspection Technologies, Alzenau, Germany

**Abstract**. The ultrasonic nondestructive testing using a conventional inspection method with a single transducer consumes large inspection time and requires a lot of man power for controlling. Phased array techniques are famous for their inspection at shorter inspection time, electronic control, their real-time applicability and sensitivity to axial and lateral resolution. These ultrasonic phased array transducers are modelled using the numerical tool called elastodynamic finite integration technique (EFIT). A 64 element phased array transducer with different operating frequencies is modelled to perform ultrasonic inspection of a steel slab immersed in water. An ultrasonic pressure wave is injected into the water with a steering angle of 18° and by mode-conversion transmits a shear wave into the steel slab with approximately 42°. A steel slab with internal notches with different depths has been simulated. A-scans are recorded for each particular element of the phased array transducer which forms a so-called parallel B-scan obtained with a single pulse-echo experiment. From the parallel B-scan a compressed A-scan is computed by averaging the A-scans in the parallel B-scan along the aperture coordinate of the phased array transducer. Modelling results are compared against measurements for selected cases.

## Introduction

The application of ultrasonic (US) phased array transducers has been proved efficient, particularly for medical diagnostics and nondestructive testing (NDT). An ultrasonic phased array transducer is composed of many single transducer elements, arranged in a fixed pattern that emit ultrasonic energy simultaneously. The phase of the excitation signal transmitted by each transducer element is used to form the excited ultrasonic wave field, for instance, the ultrasonic wave field can be steered in a certain direction. NDT techniques using a conventional transducer and a phased array transducer are illustrated in Fig. 1. Complex real-life problems can be analyzed to a great extent by numerical modelling. The elastodynamic finite integration technique (EFIT) [1], a powerful modelling tool based on the direct discretisation of the governing equations of linear elastodynamics [2], i.e., Newton-Cauchy's equation of motion and the equation of deformation rate, is used extensively in the field of NDT [3-7]. In this paper the EFIT modelling of a phased array transducer and its application are discussed. Based on these EFIT simulations the parameters of the phased array can be selected, i.e. the excitation frequency and the weighting and retardation function of each array element. As an example, the numerical modelling of an ultrasonic 64 element phased array transducer is presented. This phased array transducer is applied, for instance, to obtain a "parallel" B-scan in a single pulse-echo experiment [8]. There are many advantages of this technique, e.g., the evaluation of a large area with one shot, a high insensitivity to misalignments, and a high signal-to-noise (S/N) ratio. In Sec. 1 the modelling of the phased array transducer is elucidated in detail. The application of the phased array transducer is simulated for different frequencies and different crack parameters in Sec. 2. Sec. 3 reports a validation of the EFIT results against measurements.

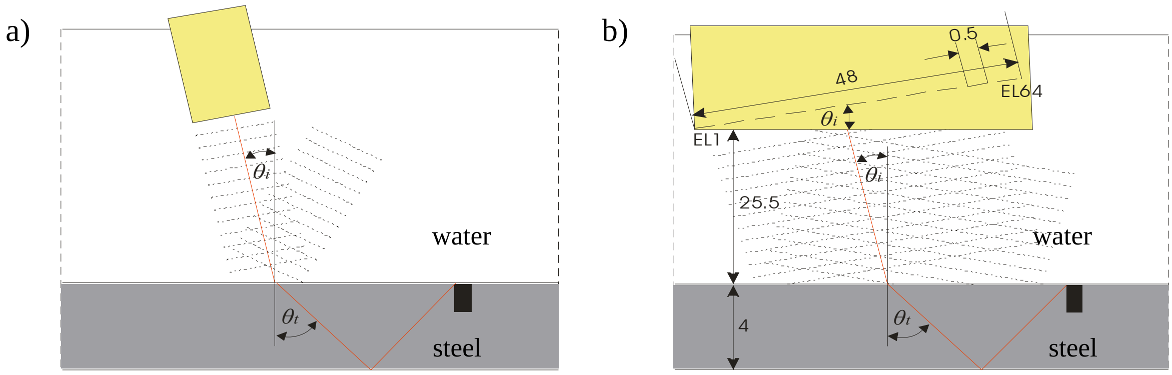


**Figure 1**: NDT of a pipeline: a) conventional ultrasonic probe, b) phased array transducer for the application of the real-time B-scan technique [8]

## 1. 2-D EFIT Modelling of Phased Array Transducer with 64 Elements

A 64 element phased array transducer with a shoe length of 48 mm is modelled using EFIT. Each transducer element in this phased array transducer has a length of 0.5 mm and a

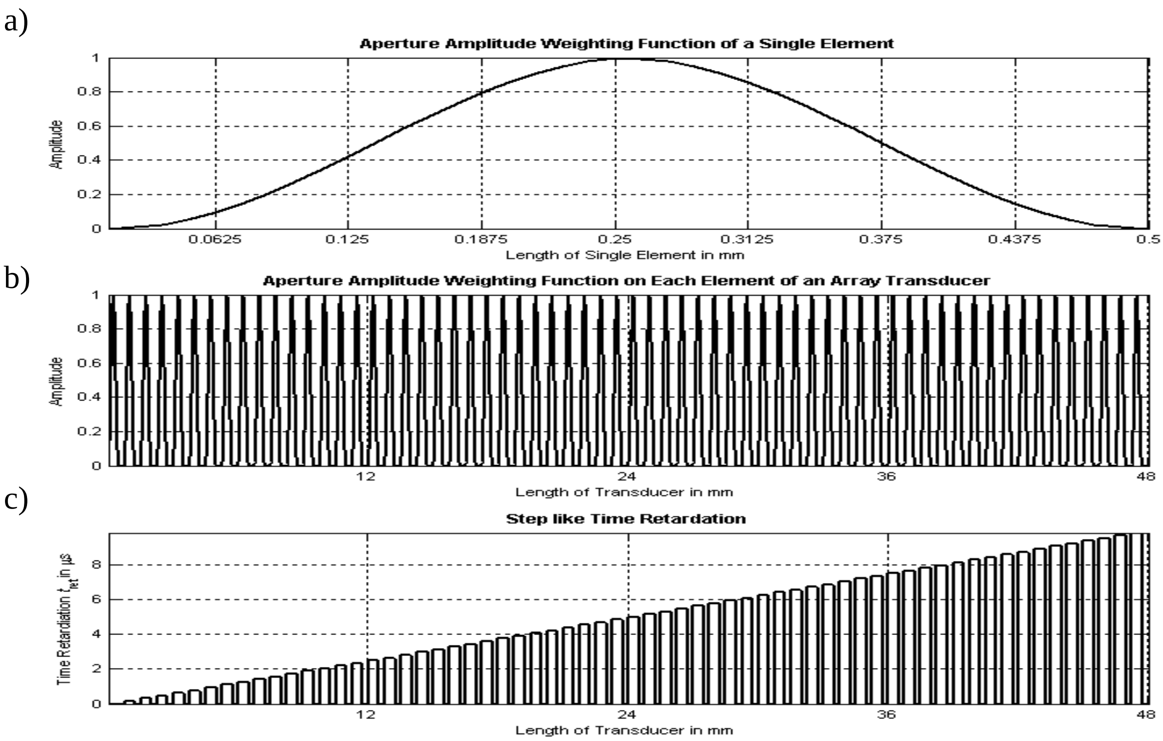


**Figure 2**: Phased array characteristics applied in the EFIT modelling: a) Tukey window function applied to each element of the 64 elements array transducer, b) a 64 element array of transducers with individual amplitude weighting function, c) step like time retardation achieved to steer the excited wave field

spacing of 0.25 mm, giving a total transducer length of 48 mm. An amplitude weighting function is applied over each transducer element as shown in Fig. 1a. The time retardation function of the phased array transducer has a step like nature to achieve a steering angle of

18°. Each transducer element in the phased array emits and receives an A-scan. The 64 A-scans form a so-called parallel B-scan [8].

## 2. Application of Phased Array Transducer

### *2.1 2-D EFIT Simulation of a Phased Array Transducer with $f_c$ = 2 MHz*

An application of the 64 element phased array transducer is illustrated in Fig. 3, where EFIT results for a steel slab with a surface breaking notch of 1 mm in depth and 0.3 mm in

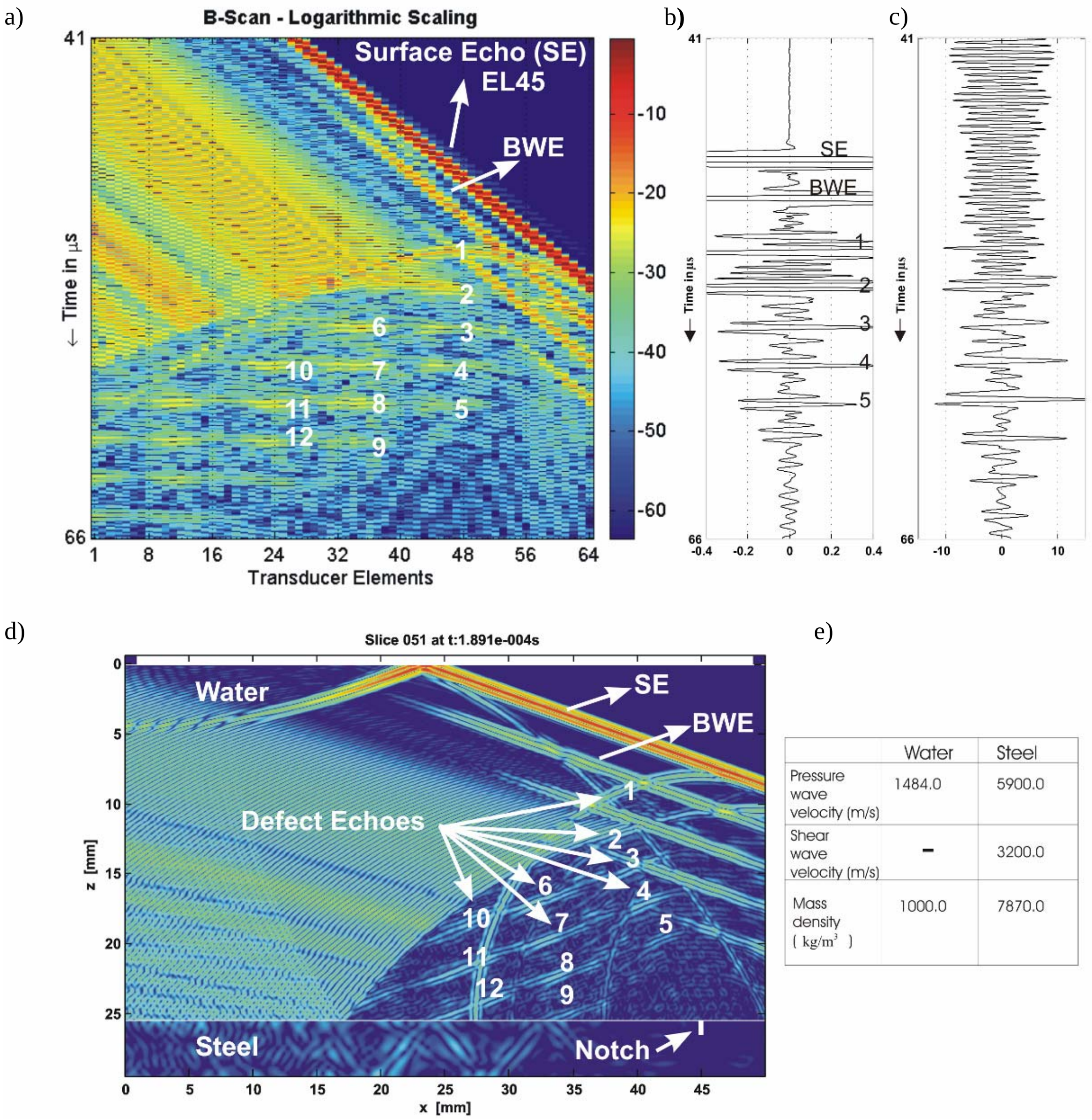


| | Water | Steel |
|---|---|---|
| Pressure wave velocity (m/s) | 1484.0 | 5900.0 |
| Shear wave velocity (m/s) | - | 3200.0 |
| Mass density ( kg/m³ ) | 1000.0 | 7870.0 |

Figure 3: 2-D EFIT results for a steel slab with a surface breaking notch of 1 mm depth and 0.3 mm width immersed in water and a 64 element phased array transducer with a carrier frequency of $f_c$ = 2 MHz: a) parallel B-scan with linear scaling and echo interpretation, b) A-scan obtained by the 45$^{th}$ element, c) A-scan obtained by averaging the A-scans of the parallel B-scan given in a), d) 2-D EFIT time-domain snapshot of the ultrasonic wave field with defect echoes, e) material parameters

width immersed in water is considered. The carrier frequency of each array element is 2 MHz. A shear wave with a transmission angle of 42° is transmitted by mode-conversion into the steel slab. The received parallel B-scan is given in Fig. 3a and an A-scan of the 45$^{th}$

element and the averaged A-scan is displayed in Fig. 3b und 3c, respectively. Each scattered wave can be interpreted in the 2-D EFIT time-domain snapshot shown in Fig. 3d. Because of the reflection from the water-steel interface and the backwall of the slab, a surface echo (SE) from the interface and a backwall echo (BWE) are received. The amplitudes of these echoes are very strong compared to the defect echoes, which are indicated in Fig. 3 by consecutive numbers. The echo 1 is the diffracted wave from the notch tip at the interface and the echoes 2-12 are reflections from the notch guided by the backwall and the steel-water interface. Fig. 3b shows the A-scan received at the 45th element. The echo amplitudes are clipped to the maximal echo amplitude in the time period of 41-66 $\mu$s. The computed A-scan in Fig. 3c is obtained by averaging the A-scans of the parallel B-scan, which indicates the defect as a sequence of echoes. Fig. 3c clearly shows the enhancement of the S/N ratio.

### *2.2 2-D EFIT Simulation of a Phased Array Transducer with* $f_c$ = 6 MHz

In this subsection the carrier frequency of the phased array transducer is increased to 6 MHz. The NDT situation is same as the previous one. Again, the echoes from the notch are indicated with numerical numbers as given in Fig. 4. In Fig. 4b the A-scan obtained by the 34th element shows defect echoes indicated with the numbers 6 to 9 which are interpreted in the parallel B-scan in Fig. 4a. The A-scan obtained by averaging the A-scans of the parallel B-scan is shown in Fig. 4c, where the S/N ratio is enhanced which makes the echo sequence clearly visible. The A-scans recorded for different notch depths are illustrated in Fig. 5. These A-scans are used for defect analysis. At lower notch depths, i.e., 0.25 mm and 0.1 mm, the echo signals are very weak even in the averaged A-scans.

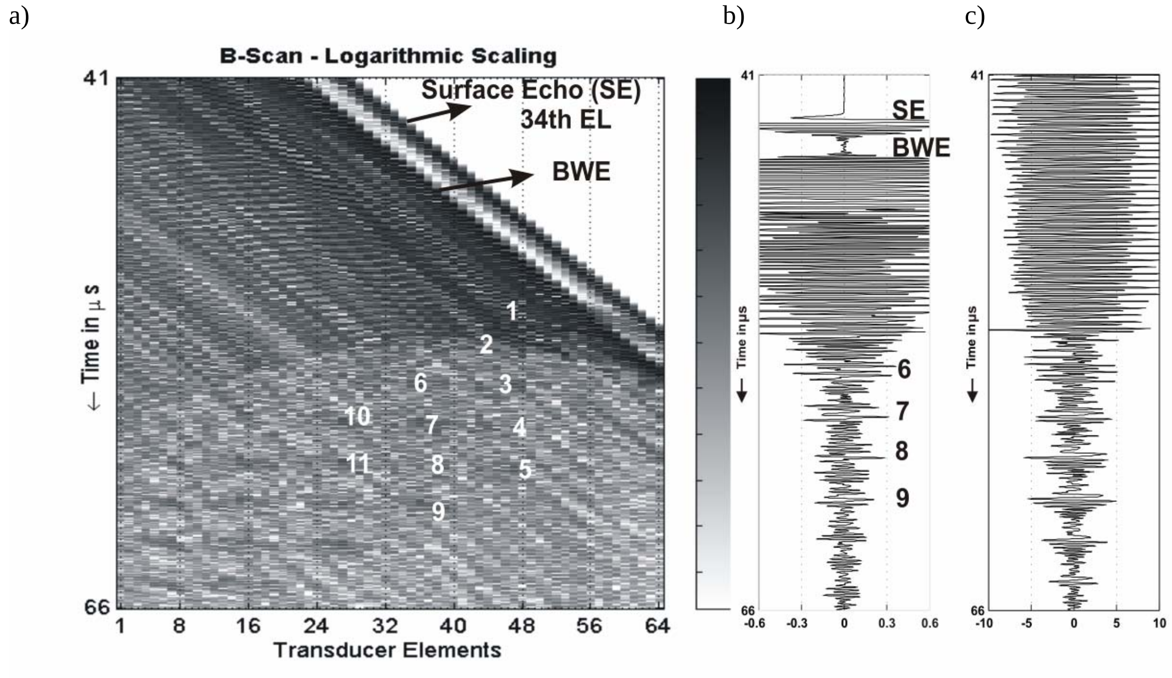


Figure 4: 2-D EFIT results for a steel slab with a surface breaking notch of 1 mm of depth and 0.3 mm of width immersed in water and a 64 element phased array transducer with a carrier frequency of $f_c$ = 6 MHz: a) parallel B-scan with linear scaling and echo interpretation, b) A-scan obtained by the 45th element, c) A-scan obtained by averaging the A-scans of the parallel B-scan given in a)

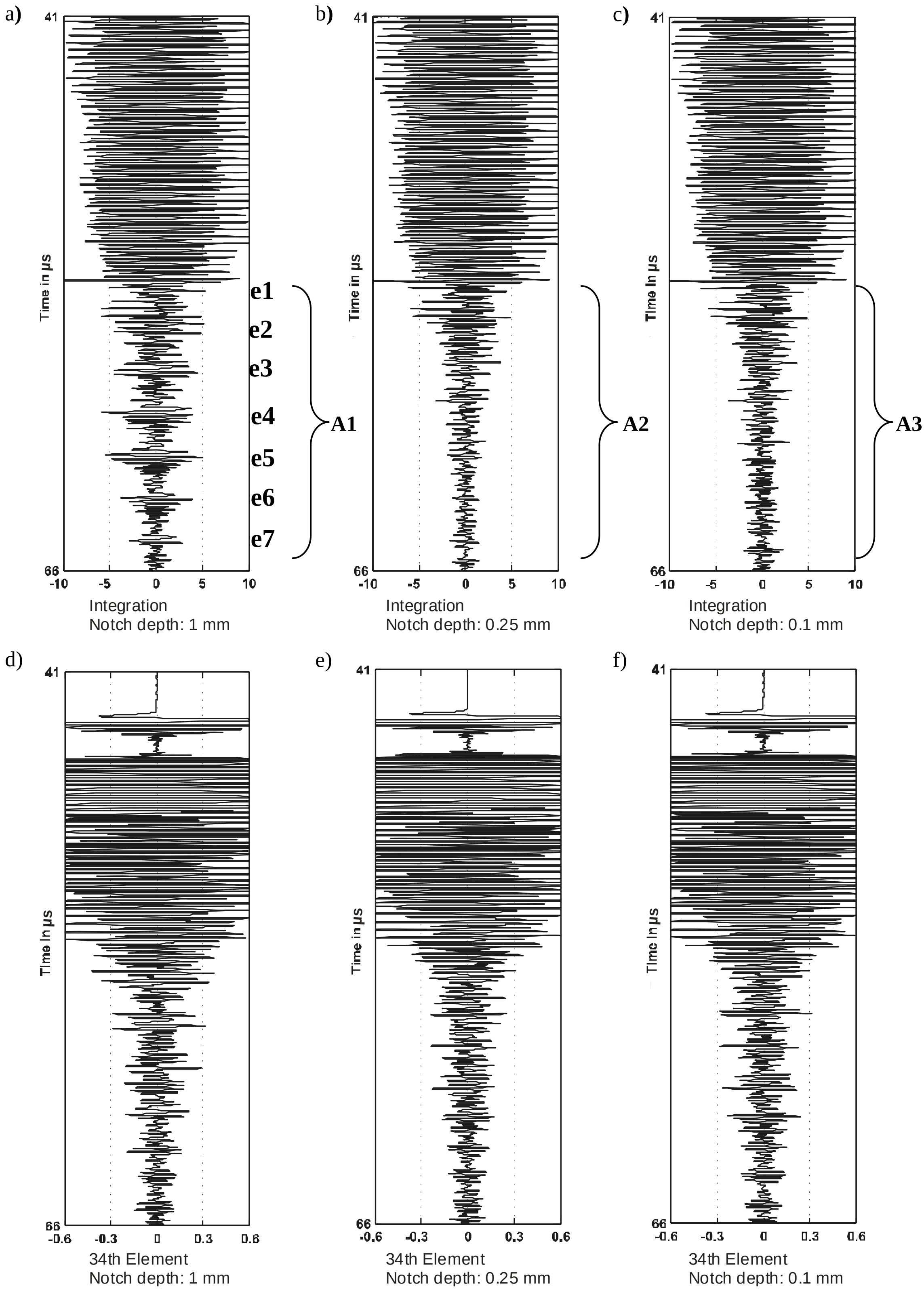


Figure 5: A-scans obtained by EFIT simulations with different notch depths. The averaged A-scans shown in a), b), and c) are obtained by averaging the A-scans in their respective parallel B-scans. The A-scans shown in d), e), and f) are the A-scans obtained by the $34^{th}$ element of the 64 element phased array transducer with different notch depths indicated under the A-scans.

## 3. Comparison of EFIT Results and Measured Data

Fig. 6 shows a comparison between the EFIT modelled and measured parallel B-scan. The EFIT result coincides with the measurement: the defect echoes like the SE echo, the BWE echo as well as the pattern of the defect echoes. In Fig. 7 the A-scans are compared: the synthetic EFIT A-scans obtained from the synthetic parallel B-scan which has the same defect echo pattern as the measured B-scan. In the 6 MHz simulations the “artificial” noise level is higher due to numerical dispersion effects, if we use the same Cartesian grid system in the EFIT modelling. This unwanted effect can be reduced by using a finer grid system.

a)

b)

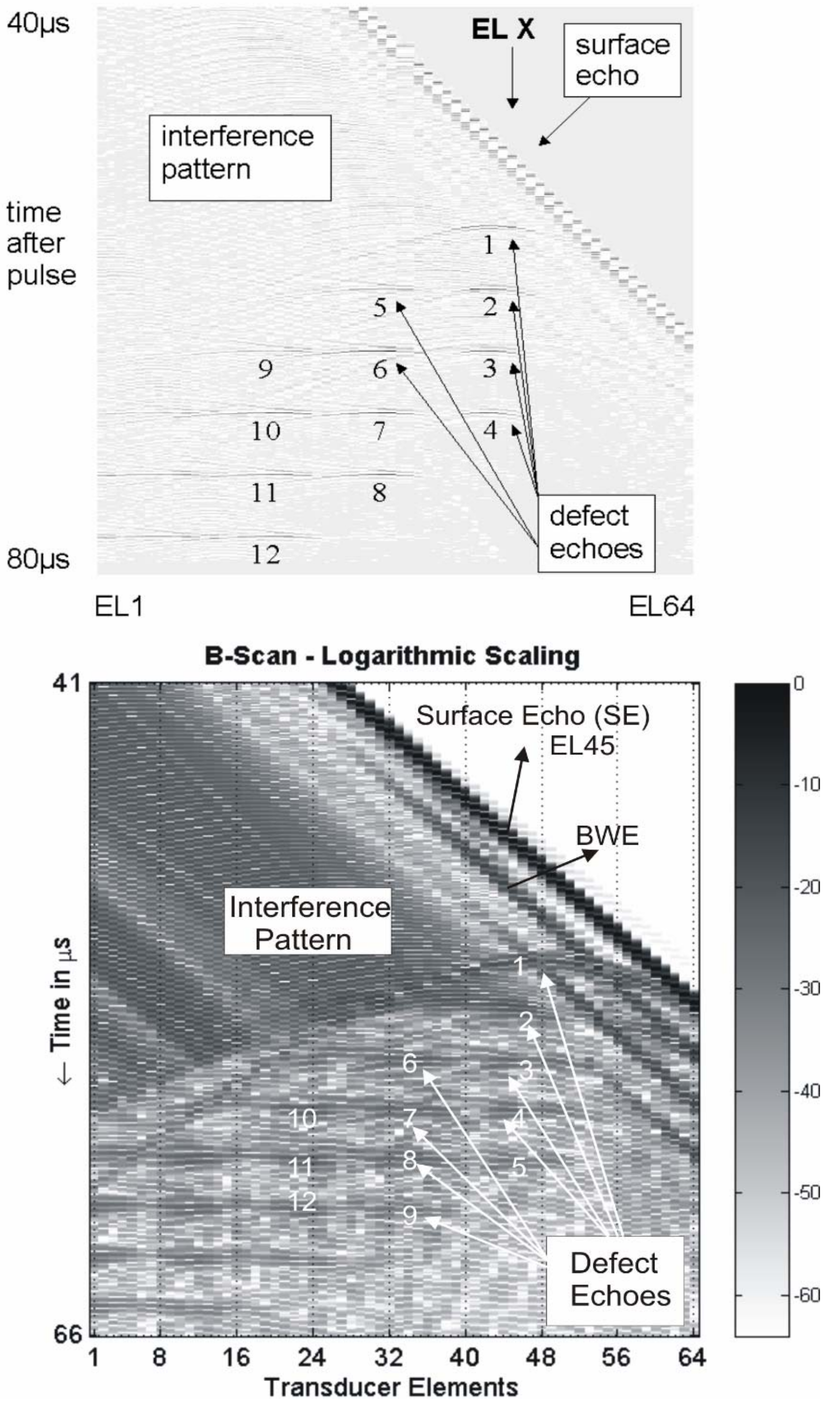


Figure 6: Comparison between measured and modelled parallel B-scan obtained with a phased array transducer: a) measured, b) modelled with 2-D EFIT applying a phased array transducer with a carrier frequency of $f_c$=2 MHz

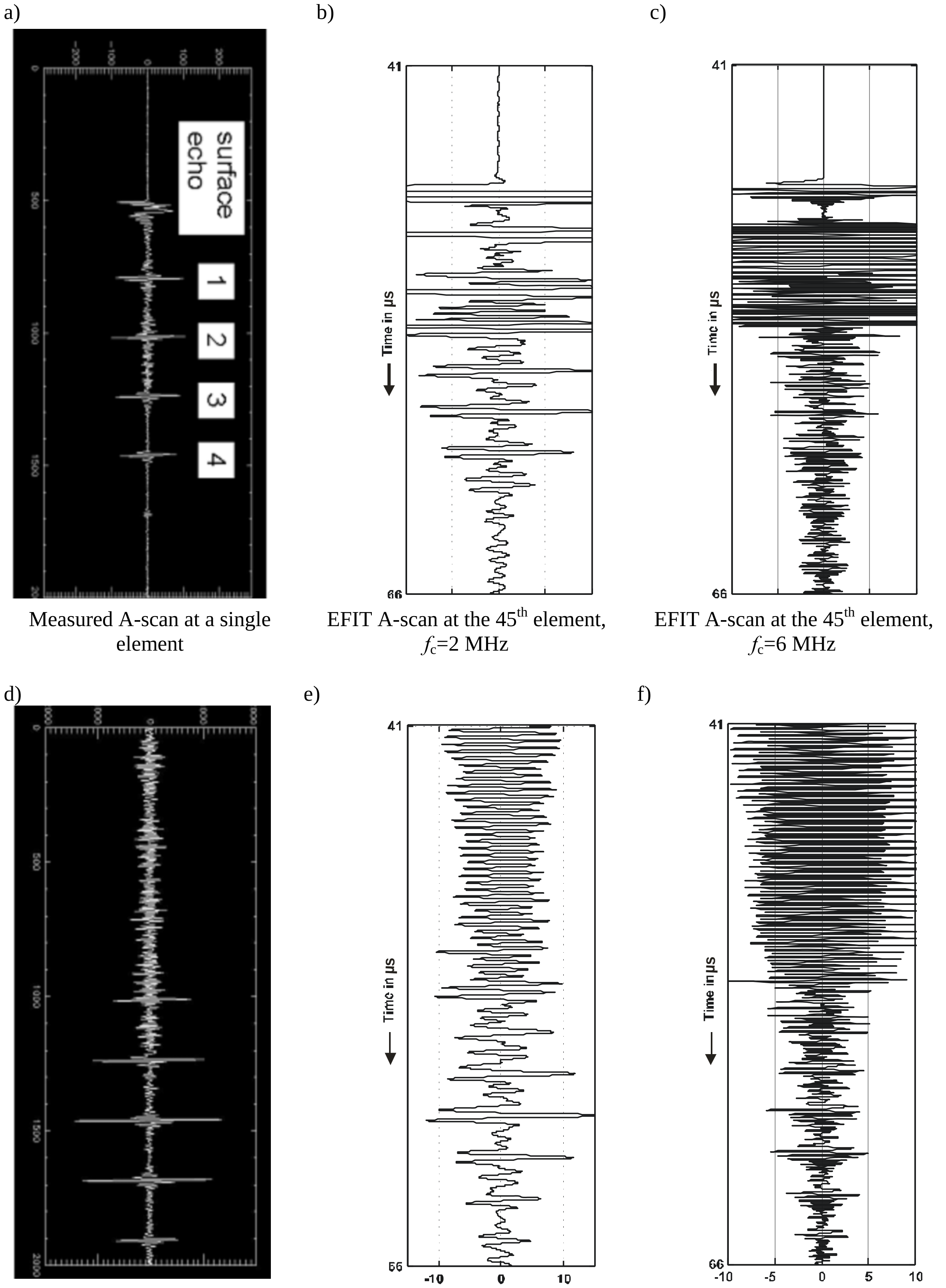


a) Measured A-scan at a single element

b) EFIT A-scan at the 45th element, $f_c$=2 MHz

c) EFIT A-scan at the 45th element, $f_c$=6 MHz

d) Measured A-scan computed from the parallel B-scan

e) Averaged EFIT A-scan computed from the parallel B-scan, $f_c$=2 MHz

f) Averaged EFIT A-scan computed from the parallel B-scan, $f_c$=6 MHz

Figure 7: Comparison of A-scans: a) and d) measured A-scan, b), c), e), f) modelled A-scan

## Conclusions

In this paper the numerical 2-D EFIT modelling of an ultrasonic 64 element phased array transducer and its application in NDT have been presented. This includes the modelling of the phased array transducer and the inspection of a slab with a surface breaking crack immersed in water. The enhancement of the signal-to-noise (S/N) ratio is clearly reproduced in the modelling results. The EFIT results have been validated against measurements. All the results are obtained for a geometry which fits into the Cartesian coordinate system. In many practical applications the surface of the test sample has a cylindrical or arbitrarily curved surface. In the future the extension of the presented modelling study to cylindrical surfaces is planned.

## References


[1] Marklein, R., 1997, *Numerical Methods for the Modelling of Acoustic, Electromagnetic, Elastic and Piezoelectric Wave Propagation Problems in the Time Domain Based on the Finite Integration Technique*, Shaker Verlag (www.shaker.de), Aachen, Germany, 1997. (in German)

[2] de Hoop, A. T., 1995, *Handbook of Radiation and Scattering of Waves.* Academic Press, London.

[3] Marklein, R., 1998, NDT Related Quantitative Modelling of Piezoelectric and Ultrasonic Phenomena, in *Proceedings of the 7th ECNDT 1998 Conference*, May 26-29, 1998, Copenhagen, Denmark, www.ndt.net/article/ecndt98/simulat/marklein/marklein.htm.

[4] Marklein, R., 2002, EFIT Simulations for Ultrasonic NDE, in *Proceedings of the 8th ECNDT 2002 Conference*, Barcelona, Spain, June 17-21, 2002, www.ndt.net/article/ecndt02/195/195.htm.

[5] Langenberg, K.-J., Mayer, K., Marklein, R., Ampha, P., Krause, M., Mielentz, F., 2004, Ultrasonic Phased Array and Synthetic Aperture Imaging in Concrete, in *Proceedings of the 16th WCNDT*, Aug. 30–Sep. 3, 2004, Montreal, Canada, www.ndt.net/article/wcndt2004/html/htmltxt/261_mayer.htm.

[6] Marklein, R., 2002, Ultrasonic Wave and Transducer Modelling with the Finite Integration Technique (FIT), in *Proceedings of the 2002 IEEE International Ultrasonic Symposium*, October 8-11, 2002, Munich, Germany.

[7] Marklein, R., 2006, Numerical Simulation of Fields and Waves in Nondestructive Testing, in *Proceedings of the 9th ECNDT 2006 Conference*, September 25-29, 2006, Berlin, Germany, these Proceedings.

[8] De Odorico, W., Koch, R., Strauss, M., Maurer, A., 2004, Real Time B-Scan-Acquisition – A Tool for High Speed and High Sensitivity Industrial On Line Inspection, in *Proceedings of the 16th WCNDT Conference*, Aug. 30–Sep. 3, 2004, Montreal, Canada, www.ndt.net/article/wcndt2004/pdf/steel/384_deodorico.pdf.